

Original Article

Evaluation of Sonochemiluminescence in a Phantom in the Presence of Protoporphyrin IX Conjugated to Nanoparticles

Ahmad Shafei¹, Ameneh Sazgarnia^{2*}, Mohammad Hassanzadeh-Kayyat³, Hossein Eshghi⁴, Samaneh Soudmand⁵, Neda Attaran Kakhki⁴

Abstract

Introduction

When a liquid is irradiated with high-intensity and low-frequency ultrasound, acoustic cavitation occurs and there are some methods to determine and quantify this phenomenon. The existing methods for performing these experiments include sonochemiluminescence (SCL) and chemical dosimetric methods. The particles in a liquid decrease the ultrasonic intensity threshold needed for cavitation onset. In this study, a new nanoconjugate made up of Protoporphyrin IX (PpIX) and gold nanoparticles (GNP), i.e., Au-PpIX was used to provide nucleation sites for cavitation. The nonradiative relaxation time of PpIX in the presence of GNPs is longer than the similar time for PpIX without GNPs. This effect can be used in medical diagnostic and therapeutic applications.

Materials and Methods

The acoustic cavitation activity was investigated studying integrated SCL signal in the wavelength range of 400-500 nm in polyacrylamide gel phantom containing luminol using a cooled CCD spectrometer at different intensities of 1 MHz ultrasound. In order to confirm these results, a chemical dosimetric method was utilized, too.

Results

SCL signal level in gel phantom containing Au-PpIX was higher than the other phantoms. These results have been confirmed by the chemical dosimetric data.

Conclusion

This finding can be related to the existence of PpIX as a sensitizer and GNPs as cavitation nuclei. In other words, nanoparticles have acted as the sites for cavitation and have increased the cavitation rate. Another theory is that activation of PpIX has produced more free radicals and has enhanced the SCL signal level.

Keywords: Cavitation, Gold Nanoparticles, Polyacrylamide Gel, Protoporphyrin IX, Sonochemiluminescence, Terephthalic Acid

1- Medical Physics and Medical Engineering Dept., Isfahan University of Medical Sciences, Isfahan, Iran

2- Medical Physics Dept., Research Centre and Department of Medical Physics, Mashhad University of Medical Sciences, Mashhad, Iran

*Corresponding author: Tel: +98 511 8002323, Fax: +98 511 8002320; email: SazgarniaA@mums.ac.ir

3- Pharmaceutics Dept., Pharmaceutical Research Center, Mashhad University of Medical Sciences, Mashhad, Iran.

4- Chemistry Dept., Ferdowsi University of Mashhad, Mashhad, Iran

5- Research Center of Medical Physics, Mashhad University of Medical Sciences, Mashhad, Iran

1. Introduction

When a liquid is irradiated with high-intensity and low-frequency ultrasound, acoustic cavitation occurs [1]. There are two types of acoustic cavitation: stable and transient. In the stable mode, the bubbles oscillate around an equilibrium radius during a considerable number of acoustic cycles without collapsing. In the transient cavitation, bubbles grow rapidly and expand to several times their original size, and violently collapse during a single acoustic compression cycle [2]. In fact, during the collapse, very high shear stresses and shock waves are produced. Moreover, very high pressure and temperature at the collapse region produce free radicals. This type of cavitation can be fatal to cells and is utilized to destroy cancer tumors [3].

There are certain methods for determining and quantifying cavitation, i.e., sonochemiluminescence (SCL) [4] and chemical dosimetric [5] methods.

Because of the opacity of the tissues, SCL detection within them is not possible [6]. Farney *et al.* proposed a polyacrylamide gel phantom for soft tissue simulation which its acoustic behavior against ultrasound is similar to soft tissues [7]. Therefore, the present study was performed on the polyacrylamide gel phantom.

When a polyacrylamide gel phantom is irradiated with high-intensity and low-frequency ultrasound, acoustic cavitation occurs. As mentioned above about the transient cavitation, very high pressure and temperature at the collapse region can produce free radicals. The extreme conditions in the interior side of the bubble also lead to the emission of light, referred to as sonoluminescence [6]. The light intensity increases significantly upon adding a small amount of luminol to the polyacrylamid gel. This emission is called SCL and results from the chemical reaction of luminol molecules with OH radicals produced within bubbles [4]. When water is sonicated, OH radicals are formed on thermolysis of H_2O . Simplified equations for production of free radicals by

collapse of cavitation in water solutions are shown in equations 1 to 4 [8].



Such chemical products may also be used to measure cavitation activity [8]. It has been shown that terephthalic acid (TA) [benzene-1, 4-dicarboxylic acid] is suitable for detecting and quantifying free hydroxyl radicals generated by the collapse of cavitation bubbles in ultrasound irradiations. During this process, TA solution, as a dosimetric solution, reacts with a hydroxyl radical generated through water sonolysis. Therefore, 2-hydroxyterephthalic acid (HTA) is produced and can be detected using fluorescence spectroscopy with an excitation and emission wavelengths of 310 and 425 nm, respectively [9].

The existence of particles in a liquid environment provides a nucleation site for the cavitation bubbles because of their surface roughness. This leads to a decrease in the cavitation threshold responsible for the increase of the quantity of bubbles, when the liquid is irradiated by ultrasound [7, 10].

Gold nanoparticles (GNPs) have been characterized as novel nanomaterials for being used in cancer therapy because of their special optical properties [11, 12]. Their low toxicity, good uptake by mammalian cells, and antiangiogenic properties make GNPs highly attractive for medical applications [13].

Protoporphyrin IX (PpIX) is an efficient hydrophobic sensitizer that is activated by both light and ultrasound waves [14]. The subsequent interaction of activated PpIX with molecular oxygen produces cytotoxic reactive oxygen species (ROS), particularly singlet oxygen ($1O_2$), which causes irreversible destruction of the target tissue [15].

The nonradiative relaxation time of PpIX in the presence of GNPs is longer than the similar time for PpIX without GNPs [16]. This long relaxation time is very favourable for the efficient generation of singlet oxygen.

In this study, the cavitation potential of PpIX conjugated to GNPs (Au-PpIX) has been studied via two methods of SCL detection in gel phantom containing luminol and chemical dosimetry at therapeutic intensities of ultrasound.

2. Materials and Methods

2.1. Preparation and characterization of Au-PpIX

Protoporphyrin IX (Sigma-Aldrich, Munich, Germany) was conjugated to the GNPs through a bidentate linker [17] as shown in Figure 1.

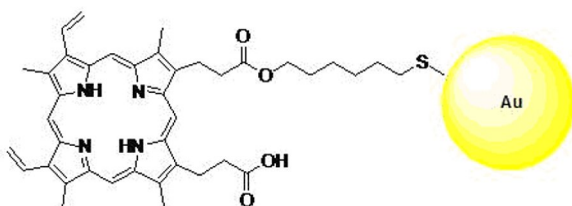


Figure 1. Protoporphyrin IX conjugated to gold nanoparticle [17]

Characterization of the GNPs was determined using two techniques: UV-visible spectrophotometry and transmission electron microscopy. The shape of nanoparticles was nearly spherical with an average diameter of 7 nm [17].

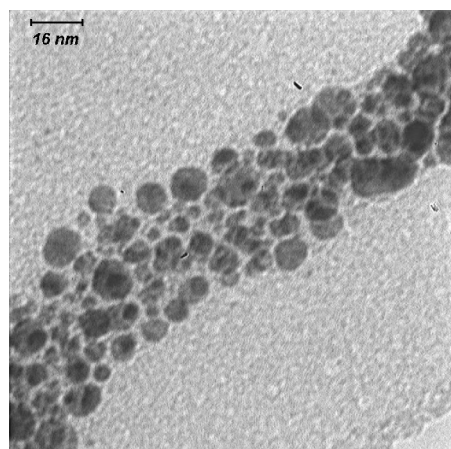


Figure 2. TEM photograph of the PpIX conjugated to gold nanoparticles

2.2. Conjugating efficiency of the PpIX to GNPs

In order to determine the conjugating efficiency of the PpIX to GNPs, the absorption intensity of PpIX conjugated to GNPs was assessed using a UV spectrophotometer and the amount of PpIX was determined [17]. Maximum absorption at 402 nm can be used for determining the PpIX content of Au-PpIX nanoconjugate. On the other hand, the amount of primary PpIX which has been entered through the construction process is also given. Therefore, the PpIX concentration conjugated to GNPs was divided by the primary PpIX concentration and the conjugating efficiency of the PpIX to GNPs was obtained. Moreover, the percentage of conjugated nanogold was calculated using atomic absorption. Therefore, the final Au-PpIX nanoconjugate contained: 42% PpIX and 58% Au [17]. Absorption spectra of PpIX and Au-PpIX in methanol are shown in Figure 3.

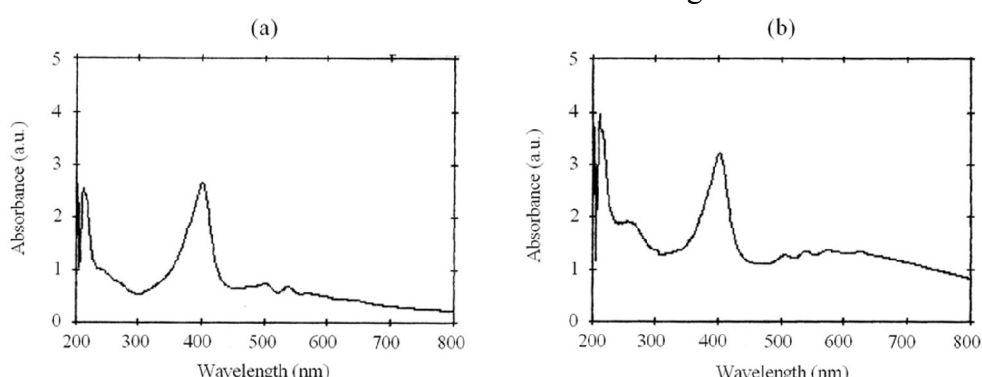


Figure 3. Absorption spectra of a) PpIX and b) Au-PpIX solutions in methanol

2.3. Ultrasound system

Ultrasound irradiation was conducted by a therapeutic ultrasound unit (215A, coproduct of Novin Medical Engineering Co, Tehran, Iran and EMS Co, Reading, Berkshire, England) in a continuous mode at a frequency of 1.1 MHz with a maximum intensity of 2 W/cm² for 3 minutes. Acoustic calibration for the power of the device was performed in a degassed water tank, using an ultrasound balance power meter (UPM 2000, Netech Corporation, Grand Rapids, MI) with uncertainty of ± 1 mW. All quoted intensities were spatial average - temporal average in our experiments. An ultrasound transducer with a surface area of 7.0 cm² was horizontally submerged in the bottom of a glass container filled with degassed water.

2.4. Cooled CCD spectrometer

The SCL signal was detected using a cooled electro-optic spectrometer (Thermo-Electric cooled and regulated CCD, Avantec Co., NL-6961 RB Eerbeek, The Netherlands). The AvaSpec-2048×14 Fiber Optic Spectrometer is a back-thinned type CCD spectrometer with high quantum efficiency and high UV sensitivity. The spectrometer was equipped with a fiber optic entrance connector (standard SMA), a collimating and focusing mirror, and a diffraction grating.

2.5. Polyacrylamide gel preparation

The polyacrylamid gel was formed by the procedure stated by Khokhlova et al [18]. 9.735 g of acrylamide and 0.265 g of bis-acrylamide (Sigma, Aldrich, Munich, Germany) were dissolved in 50 ml of deionized water. The addition of a polymerizing initiator of 0.02 g of ammonium persulfate and 0.2 ml of TEMED (Sigma, Aldrich, Munich, Germany) created a 7% acryamide gel. The gel was poured into a mould (4×4×8 cm³) and allowed to polymerize under vacuum. The transmission spectrum of polyacrylamid gel is shown in Figure 4.

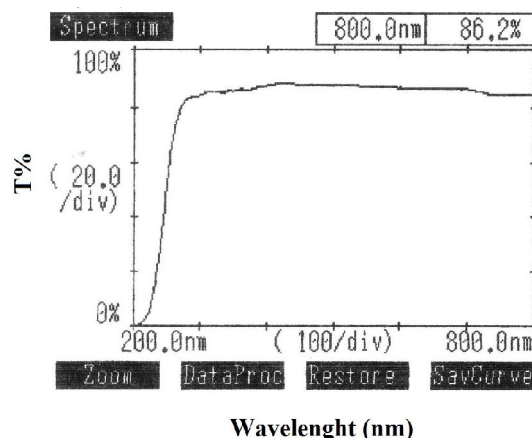


Figure 4. Transmission spectrum of the polyacrylamide gel.

2.6. Luminol solution preparation

0.041 g of luminol (5-amino-2, 3-dihydrophthalazine-1,4-dione) (Sigma, Aldrich, Munich, Germany) and 85.23 g of sodium carbonate (Sigma, Aldrich, Munich, Germany) were dissolved in 500 ml of deionized water [4].

2.7. Experimental protocol for sonochemiluminescence detection

A container with dimensions of 10×8×16 cm³ was constructed from black Perspex (PMMA) slabs of 5 mm thickness. A quartz window was designed in one side of the container in order to transmit emitted light. A band-pass filter (FWHM= 325-475 nm) was put on the quartz window. A 400-micron fiber optic equipped with special connectors was used to transfer light from the phantom to the spectrometer. The ultrasound probe was placed under the phantom through a specially designed hole in the floor of the container. The container was filled with degassed distilled water thermostated at 18 °C. In order to prevent successive reflections of ultrasound waves, a layer of foam was pasted inside the container on the floor and the walls. Black Perspex slabs sealed the phantom from background light. Cavitation detection was conducted in a phantom made of a transparent polyacrylamide gel.

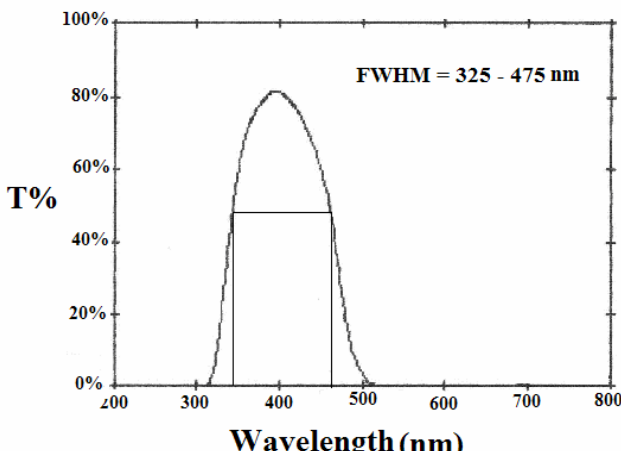


Figure 5. Band pass filter (B-390) with FWHM= 325-475 nm

In this study, the experiments were performed on four similar blocks of gel: gel containing PpIX (0.12 mg/ml), gel containing GNPs (0.22 mg/ml), gel containing Au-PpIX (0.39 mg/ml), and simple gel. It should be noted that PpIX, GNPs, and Au-PpIX were injected into the gel's blocks 5 minutes before the measurements. The experimental apparatus is shown in Figure 6.

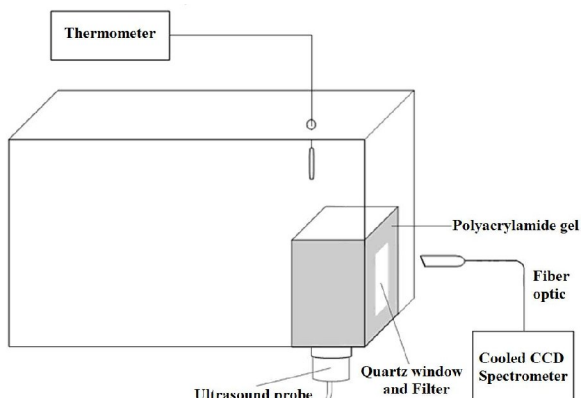


Figure 6. Experimental setup used for sonochemiluminescence recording.

First, the gel's block was put in a special place in the back of the quartz window into the container. The ultrasonic probe was inserted beneath the gel and the SCL spectrum was taken for 10 sec. These steps were repeated three times for each gel in ultrasonic intensities of 0.5, 1, and 2 W/cm² (ISATA) in a continuous mode.

The SCL signal in four different gel phantoms was recorded in wavelength range between

400 and 500 nm and the integrated signal was calculated.

2.8. Preparation of terephthalic acid solution

The dosimetry solution of terephthalic acid (TA) was prepared according to the standard protocols [8] containing TA (2 mmol/L, Aldrich) in almost 800 ml deionized water and then treated with 5 ml NaOH (1 M). The solution was stirred for about one hour [8] and kept in a cool and dark place (4 °C) to prevent photochemical reactions. A cylindrical chamber was constructed from PVC in order to sonicate the TA solution (5 cm³). The floor of chamber was made of a thin acoustically transparent parafilm layer.

2.9. Experimental protocol of chemical dosimetry

The chamber containing TA solution was located in a container filled with degassed water in the near-field of the ultrasonic probe at 5 mm away from the surface of the probe. To perform experiments under progressive-wave conditions and free of acoustic reflection, the inner surfaces of the container were covered by foam [8]. Sonication time of TA solution was selected as 20 min. With this setting, the maximum increase in temperature was 3 °C. The measurements were performed on four TA solutions: TA solution containing PpIX (0.12 mg/ml), TA solution containing GNP (0.22 mg/ml), TA solution containing Au-PpIX (0.39 mg/ml), and TA solution without particles. After ultrasound exposure on each solution, the fluorescence signal was recorded using a spectrofluorimeter (FP-6200, Jasco, Japan) with excitation and emission of wavelengths of 310 and 420 nm, respectively. The irradiated solutions were kept in a dark place through the experiment and fluorometric assessments were done within 2-4 hr after sonication. Before ultrasound irradiation, the fluorescence signal of solutions was also measured. Each experiment was repeated three times.

2.10. Data analysis

All statistical analyses were performed using SPSS statistical software version 13.0 (SPSS Inc, Chicago, IL). According to the Kolmogorov-Smirnov normality test, the data distribution was normal. Consequently, the paired sample t-test was used to compare the intensities of 1 and 2 W/cm² with a confidence level of 95%. The integrated SCL signal between different gel phantoms was also compared using one-way analysis of variance. Data is presented as mean \pm SD. A p<0.05 was considered as statistically significant.

3. Results

An example of the recorded SCL signals in different polyacrylamide gel phantoms following 1 MHz ultrasonic irradiation with 2

W/cm² intensity in a continuous mode in the range of 220-800 nm is presented in Figure 7. As shown in Figure 6, the highest SCL signals were recorded in the gel phantoms containing Au-PpIX, GNP and PpIX, respectively.

In all SCL signal measurements, the level of background noise (dark signal) was recorded and subtracted from the SCL signal.

The SCL signals were recorded in the wavelength range of 400-500 nm in four different gel phantoms using a certain filter (FWHM= 375-500 nm). The mean and standard deviation of the SCL signal following ultrasonic irradiation in 0.5, 1, and 2 W/cm² intensities in continuous mode and in different polyacrylamide gel phantoms are presented in Figure 8.

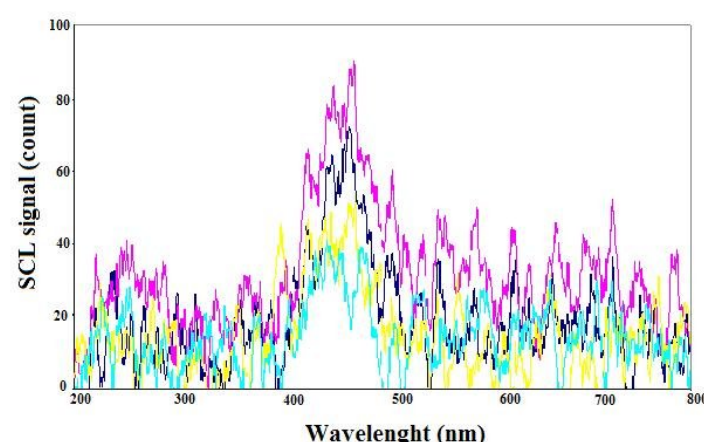


Figure 7. Example of recorded SCL signals in different polyacrylamide gel phantoms containing luminol following 1 MHz ultrasonic irradiation with 2 W/cm² intensity in continuous mode at the range of 220-800 nm. In this figure, signals in pink, blue, yellow, and green are related to gel phantoms containing Au-PpIX, GNP, PpIX, and gel phantom without GNP, respectively.

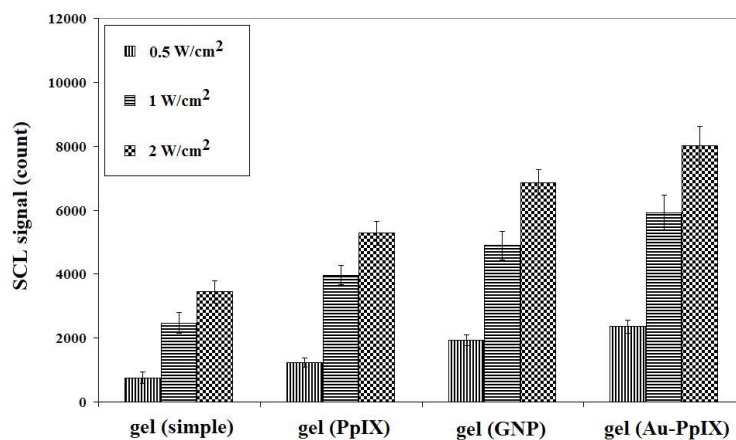


Figure 8. Mean \pm SD of the recorded SCL signals in different polyacrylamide gel phantoms following irradiation of 0.5, 1, and 2 W/cm² ultrasound waves in continuous mode in the wavelength range of 400-500 nm.

Statistical comparison of the results showed a significant difference in the recorded SCL signal following irradiation of 0.5 and 1 W/cm² ultrasound waves in the continuous mode between the gel phantoms containing nanoparticles (GNP and Au-PpIX) and the gel phantoms without nanoparticles (PpIX and simple) ($p<0.04$). However, there was no significant difference in the recorded SCL signal between the gel phantoms containing Au-PpIX and GNP ($p>0.2$).

Our results showed a significant difference in the SCL signal recorded following irradiation of 2 W/cm² ultrasound waves between all gel phantoms ($p<0.04$).

Figure 8 shows that any increase in the intensity of the sonication is associated with an increase in the SCL signal in different gel phantoms.

A significant difference in the SCL signal between 2 W/cm² intensity and 0.5 and 1

intensities was observed in gel phantoms containing Au-PpIX, GNP, and PpIX ($p<0.04$), but the SCL signal related to gel phantom without particles did not show a significant difference between 1 and 2 W/cm² intensities ($p=0.183$).

Hydroxyl radical production was measured in the field of 1 MHz ultrasound waves at 0.5, 1, and 2 W/cm² intensities in continuous mode and in the temperature of 18-20 °C by the TA dosimetric method.

Figure 9 shows the fluorescence signals in the different TA solutions containing Au-PpIX, GNP, PpIX, and gel without particles following irradiation of 0.5, 1, and 2 W/cm² ultrasound waves in continuous mode (excitation wavelength=310 nm, emission peak wavelength=420 nm, emission and excitation band width=5 nm, sonication=20 min).

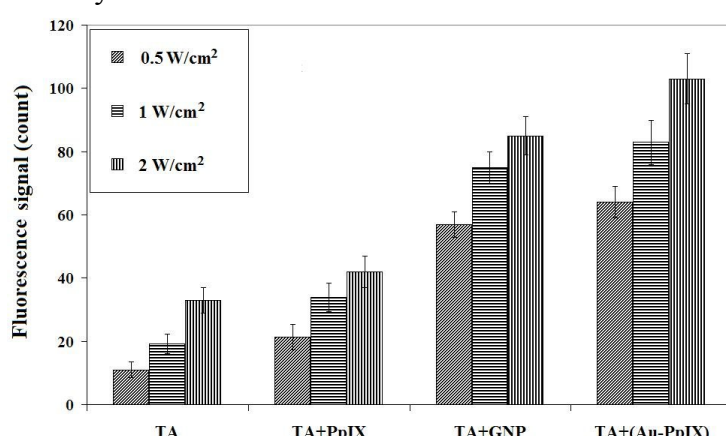


Figure 9. Mean±SD of the fluorescence signal in different TA solutions containing Au-PpIX, GNP, PpIX and gel without particles following irradiation of 0.5, 1, and 2 W/cm² ultrasound waves in continuous mode in the temperature of 18-20 °C (excitation wavelength=310 nm, emission peak wavelength=420 nm, emission and excitation band width=5 nm, sonication time=20 min).

As it is observed in Figure 9, the highest fluorescence signals were recorded in different TA solutions containing Au-PpIX, GNP, and PpIX, respectively.

Statistical comparison of the results showed a significant difference in the fluorescence signal recorded following irradiation of 0.5, 1, and 2 W/cm² ultrasound waves in continuous mode between the TA solutions containing nanoparticles (GNP and Au-PpIX) and the TA solutions without nanoparticles (PpIX and

simple) ($p<0.05$), but there was no significant difference in the fluorescence signal between the TA solutions containing Au-PpIX and GNP ($p>0.1$).

Our results showed that the fluorescence intensity in the TA solution containing Au-PpIX following irradiation of 2 W/cm² ultrasound waves was significantly different in comparison with the other solutions ($p<0.05$).

Figure 9 shows that any increase in the intensity of the sonication is associated with an

increase in the fluorescence signal in all phantoms.

4. Discussion and Conclusion

Many clinical methods for cancer treatment are not target-based and researchers are looking for good approaches to treat cancer that focus on the tumor area with minimal damage to the healthy tissues [19]. One of the noninvasive therapeutic applications of ultrasound that has been considered in the recent years is sonodynamic therapy (SDT), which is a physical treatment that uses ultrasound waves with a sonosensitizer [20]. In SDT, activated sensitizer molecules provide cytotoxicity when exposed to ultrasound. The activation of the sensitizer depends on cavitation, and therefore high intensity ultrasound is an important necessity. Besides, high intensity ultrasound can impose side effects on the healthy tissues surrounding the tumor [21]. There is a considerable interest in the evaluation of cavitation for possibility of SDT which uses low level ultrasound to enhance the action of the sonosensitizers *in vivo*. There exist certain methods for determining and quantifying cavitation. In our research, the methods for performing these experiments included SCL [7] and chemical dosimetric [8].

In the present study, we have investigated the cavitation potential of the Au-PpIX nanoparticles, which have been recently employed for sonodynamic therapies.

The first method was executed on the polyacrylamide gel phantom containing luminol. When the gel is irradiated by ultrasound, gas bubbles and transient cavitation occurs in the gel. Following the collapse of the bubbles, free radicals are produced and then the SCL is emitted from the chemical reaction of luminol molecules with OH radicals produced by transient cavitation [4]. Farny *et al.* worked on the polyacrylamid gel for modeling biological systems because it has some physical and chemical properties on soft tissues against ultrasound [7].

In the second method, we also utilized TA as a chemical dosimeter to quantify the free hydroxyl radicals generated by collapsing of the transient cavities produced by low-level intensity ultrasound. This dosimetry is based on the fluorometric method which is very sensitive to hydroxyl radical measurement [9]. Barati *et al.* showed that the TA dosimetry is suitable for detecting and quantifying free hydroxyl radical as a criterion for cavitation production in medical ultrasound fields [8]. The results of the recorded SCL signal in different gel phantoms were confirmed by the dosimetric data.

On the basis of our results, the SCL signal level in the gel phantom without particles was lower than the phantoms containing GNP, PpIX, and Au-PpIX. When the gel phantom containing PpIX is irradiated by ultrasound waves, cavitation occurs. During cavitation collapse, the extremely high temperature and pressure provide a favorable condition for the occurrence of chemical reactions and production of free radicals. Afterward, through the chemical reaction of luminol molecules with OH radicals, SCL is emitted. Moreover, these free radical molecules are in high energy state and this energy could be transferred to the PpIX molecules to form PpIX in an excited state. The energy transfer from activated PpIX to oxygen molecules can produce singlet oxygen and the cytotoxicity of sonosensitization in biological tissues is intermediated by this molecule.

Our results showed that SCL signal in phantom containing Au-PpIX is higher than the other phantoms. This finding can be related to the existence of PpIX as a sensitizer and GNPs as the cavitation nuclei. In other words, maybe nanoparticles act as sites for cavitation and increase the cavitations' rate. Or perhaps activation of PpIX has produced more free radicals and has enhanced the SCL signal level. Since there is a significant difference in the SCL signal between the phantom containing GNP and the phantom without particles, the first assumption could be confirmed.

Tuziuti et al. showed that the existence of particles in a liquid provides a nucleation site for the cavitation bubble due to their surface roughness, and it leads to a decrease in the cavitation threshold responsible for the increase in the quantity of bubbles, when the liquid is irradiated by ultrasound [10].

Our results showed that the fluorescence signal in the TA solution containing Au-PpIX was higher than that in the other solutions. This finding could be related to several reasons: (1) GNPs acted as cavitation nuclei, i.e., the nanoparticles may have acted as the sites for cavitation and increased the cavitation rate [10], (2) the PpIX acted as sonosensitizers and activation of the PpIX has produced more free radicals and the chemical reaction of luminol molecules with OH radicals has enhanced the SCL signal level [4], and (3) increased collapse of cavities could be caused by another possible process.

Experimental results obtained by sonication of the TA solutions have indicated that the ultrasound irradiation parameters such as intensity and nucleation sites for bubble generation are effective in hydroxyl radical production and in turn, in the production of cavitation.

In conclusion, a novel nanoconjugate composition of PpIX and GNPs (Au-PpIX) is introduced as a promising compound and a new sonosensitizer for SDT.

Acknowledgment

The authors would like to thank the research deputy of Mashhad University of Medical Sciences for financial support of this research. This paper has been extracted from a PhD thesis of medical physics.

References

1. Hodnett M, Zequiri B. A detector for monitoring the onset of cavitation during therapy-level measurements of ultrasonic power. *J phys Conf Ser.* 2004;1(1):112-7.
2. Tang H, Wang CC, Blankschtein D, Langer R. An investigation of the role of cavitation in low-frequency ultrasound-mediated transdermal drug transport. *Pharm Res.* 2002;19(8):1160-9.
3. Marmottant P, Hilgenfeldt S. Controlled vesicle deformation and lysis by single oscillating bubbles. *Nature.* 2003;423(6936):153-6.
4. McMurray HN, Wilsom BP. Mechanistic and spatial study of ultrasonically induced luminal chemiluminescence, *J Phys Chem.* 1999;103(20):3955-62.
5. Hasanzadeh H, Mokhtari-Dizaji M, Bathaei SZ, Hassan ZM. Evaluation of correlation between chemical dosimetry and subharmonic spectrum analysis to examine the acoustic cavitation. *Ultrason Sonochem.* 2010;17(5):863-9.
6. Daniels S, Price DJ. Sonoluminescence in water and agar gels during irradiation with 0.75 MHz continues-wave ultrasound. *Ultrasound Med Biol.* 1991;17(3):297-308.
7. Farney CH, Wu T, Holt G, Murray TW, Roy RA. Nucleating cavitation from laser-illuminated nanoparticles, *Acoust Res Lett.* 2005;6(3):138-43.
8. Barati AH, Mokhtari M, Mozdaran H, Bathaei H, Hassan ZM. Free hydroxyl radical dosimetry by using 1 MHz low level ultrasound waves. *Iran J Radiat Res.* 2006;3(4):163-9.
9. Haosheng C, Jiadao W, Darong C. Cavitation damages on solid surfaces in suspensions containing spherical and irregular microparticles. *Wear.* 2009;266(1-2):345-8.
10. Tuziuti T, Yasui K, Sivakumar M, Iida Y, Miyoshi N. Correlation between cavitation noise and yield enhancement of sonochemical reaction by particle addition. *J Phys Chem A.* 2005;109(21):4869-72.
11. Huang X, Jain PK, El-Sayed IH, El-Sayed MA. Plasmonic photothermal therapy (PPTT) using gold nanoparticles. *Lasers Med Sci.* 2008;23(3):217-28.
12. Paciotti GF, Myer L, Weinreich D, Goia D, Pavel N, McLaughlin RE, et al. Colloidal gold: a novel nanoparticles vector for tumor directed drug delivery. *Drug Deliv.* 2004;11(3):169-83.
13. Kah JC, Olivo MC, Lee CG, Sheppard CJ. Molecular contrast of EGFR expression using gold nanoparticles as a reflectance-based imaging probe. *Mol Cell Probes.* 2008;22(1):14-23.

14. Liu Q, Wang X, Wang P, Xiao L, Hao Q. Comparison between sonodynamic effect with protoporphyrin IX and hematoporphyrin on sarcoma 180. *Cancer Chemother Pharmacol*. 2007;60(5):671-80.
15. Li B, Moriyama EH, Li F, Jarvi MT, Allen C, Wilson BC. Diblock copolymer micelles deliver hydrophobic protoporphyrin IX for photodynamic therapy. *Photochem Photobiol*. 2007;83(6):1505-12.
16. Jimenez Perez JL, Orea AC, Gallegos ER, Fuentes RG. Photoacoustic Spectroscopy to determine in Vitro the non radiative relaxation time of porotoporphyrin IX solution containing gold metallic nanoparticles. *Eur Phys J Spec Top*. 2008;153(1): 353-6.
17. Eshghi H, Attaran N, Sazgarnia A, Mirzaie N, Shanei A. Synthesis and Characterization of New Designed Protoporphyrin-Stabilized Gold Nanoparticles for Cancer Cells Nanotechnology-Based Targeting. *Int J Nanotechnol*. 2011;8(8-9):700-11.
18. Khokhlova VA, Bailey MR, Reed JA, Cunitz BW, Kaczkowski PJ, Crum LA. Effects of nonlinear propagation, cavitation and boiling in lesion formation by high intensity focused ultrasound in a gel phantom. *J Acoust Soc Am*. 2006;119(3):1834-48.
19. Kuroki M, Hachimine K, Abe H, Shibaguchi H, Kuroki M, Maekawa S, et al. Sonodynamic therapy of cancer using novel sonosensitizers. *Anticancer Res*. 2007;27(6A):3673-7.
20. Jin ZH, Miyoshi N, Ishiguro K, Umemura S, Kawabata K, Yumita N, et al. Combination effect of photodynamic and sonodynamic therapy on experimental skin squamous cell carcinoma in C3H/HeN mice. *J Dermatol*. 2000;27(5):294-306.
21. Clement GT. Perspectives in clinical uses of high intensity focused ultrasound. *Ultrasonics*. 2004;42(10):1087-93.